Available online at www.sciencedirect.com
SCIENCE DIRECT®
Journal of Nuclear Materials 337–339 (2005) 124–128
journal of nuclear materials
www.elsevier.com/locate/jnucmat

# DIVIMP modeling of the toroidally symmetrical injection of $^{13}CH_4$ into the upper SOL of DIII-D

A.G. McLean [a,*], J.D. Elder [a], P.C. Stangeby [a], S.L. Allen [c], J.A. Boedo [g], N.H. Brooks [b], M.E. Fenstermacher [c], M. Groth [c], S. Lisgo [a], A. Nagy [d], D.L. Rudakov [g], W.R. Wampler [e], J.G. Watkins [e], W.P. West [b], D.G. Whyte [f]

[a] *Institute for Aerospace Studies, University of Toronto, 4925 Dufferin Street, Toronto, Ont., Canada M3H 5T6*
[b] *General Atomics, P.O. Box 85608, San Diego, CA 92186-5608, USA*
[c] *Lawrence Livermore National Laboratory, P.O. Box 808, Livermore, CA 94551, USA*
[d] *Princeton Plasma Physics Laboratory, Princeton, NJ 08543, USA*
[e] *Sandia National Laboratory, P.O. Box 5800, Albuquerque, NM 87185, USA*
[f] *University of Wisconsin, Madison, WI 53706, USA*
[g] *University of California, San Diego, La Jolla, CA 92093-0417, USA*

**Abstract**

As part of a study of carbon–tritium co-deposition, we carried out an experiment on DIII-D involving a toroidally symmetric injection of $^{13}CH_4$ at the top of a LSN discharge. A Monte Carlo code, DIVIMP-HC, which includes molecular breakup of hydrocarbons, was used to model the region near the puff. The interpretive analysis indicates a parallel flow in the SOL of $M_{\|} \sim 0.4$ directed toward the inner divertor. The $CH_4$ is ionized in the periphery of the SOL and so the particle confinement time, $\tau_c$, is not high, only ~5 ms, and about 4X lower than if the $CH_4$ were ionized at the separatrix. For such a wall injection location, however, approximately 60–75% of the $CH_4$ gets ionized to $C^+$, $C^{2+}$, etc., and is efficiently transported along the SOL to the inner divertor, trapping hydrogen by co-deposition there.


*PACS:* 52.20.–j; 52.25.Vy; 52.65.–y; 52.65.Pp
*Keywords:* Carbon impurities; DIII-D; DIVIMP; Edge modeling; Hydrocarbons

## 1. Introduction

Carbon is commonly used for first wall and divertor target coverage, and since it is susceptible to chemical sputtering, studies have been carried out on most tokamaks using injection of known flow rates of methane to evaluate the magnitude and characteristic radiative emissions associated with chemical sputtering. Ref. [1] provides an extensive set of references for methane injection experiments including studies on core carbon transport, plume characterization, erosion and re-deposition, molecular break-up studies, and evaluation of carbon penetration through the SOL to the core.

On DIII-D we carried out an experiment [2] involving the injection of $^{12}CH_4$ and $^{13}CH_4$ at the top of the torus, similar to one carried out on JET [3], to study certain aspects of the carbon–tritium co-deposition process, which can have serious implications for tritium retention in

* Corresponding author.
*E-mail address:* adam.mclean@utoronto.ca (A.G. McLean).

0022-3115/$ - see front matter © 2004 Elsevier B.V. All rights reserved.
doi:10.1016/j.jnucmat.2004.10.130

ITER. In this experiment care was taken to make the injection toroidally symmetric, aiding the interpretation: $CH_4$ injection was through the upper outer pumping plenum (Fig. 1) – thus justifying the standard, but often not satisfied, code assumption of symmetry. Based on the earlier $^{13}CH_4$ puffing experiments on JET, it is believed that a large scale convective pattern in the SOL, which transports wall-released C (whether due to wall sputtering or puffed, as here) poloidally over the top of the closed flux surfaces, and down along the centrepost and into the inner divertor, led to the observation of strong retention of tritium in the inner divertor of JET and very little in the outer divertor [4]. One of the objectives of the present experiment was to obtain direct visual confirmation of this poloidal convection pattern using toroidal cameras and vertical filterscopes viewing the injection region. A second objective was to establish the efficiency with which wall-released methane is converted to C-ions (i.e., not being lost back to local solid surfaces as neutral and charged molecular fragments). One of the main contributors to C subsequently appearing in H/D/T co-deposits may be chemical sputtering of the walls. The efficiency of penetration of carbon is likely to be much higher for wall sources than for release from divertor targets where prompt local re-deposition can be strong due to the local fast, strongly collisional plasma flow to the targets. A third objective was to measure the efficiency of core contamination of such a toroidally symmetric wall source, i.e., the impurity confinement time.

A methane-break-up module has been added to the OEDGE [5] (DIVIMP) code in order to interpretively model the results of the injection of $CH_4$ into DIII-D [6].

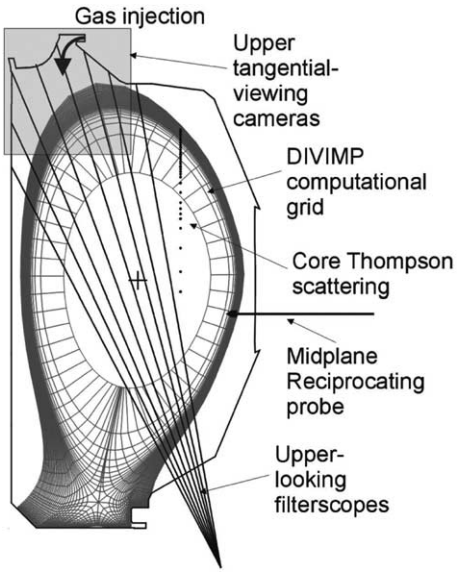


Fig. 1. Gas injection arrangement, specific diagnostics used and computational grid.

## 2. Experiment and modeling

The experiment was carried out over 2 days. Ordinary $^{12}CH_4$ was used on the first – 'plasma characterization' – day, with many repeat shots to maximize edge diagnosis. The rate of injection, 4.4 tl/s (0.59 pa $m^3$/s), was established by adjustment to achieve an approximate 35% increase of core carbon density over 500 ms, as measured by charge exchange recombination (CER) spectroscopy (CVI), over the no-injection base. This condition was chosen to give a large enough injection rate to get measurable effects without disturbing the plasma. The fact that the injection was not localized – but was distributed in a toroidally symmetric way – greatly helped to reduce the risk of significantly changing the plasma at the location where the gas entered – which is the most critical location. (In any case, if the plasma did change, this could be monitored using the toroidally localized diagnostics, such as Thomson scattering, and taken into account in the analysis.) Injections lasted for 3.0 s in each discharge, beginning after stable L-mode conditions were achieved. The $^{13}CH_4$ puffing was repeated over a series of 22 consecutive identical discharges on the second day. More details of the experiment are provided in [2]. The $^{13}C$ deposits were found to be almost entirely on the inner divertor target within the sensitivity and depth resolution of the ion beam analysis technique used [7]. The deposition pattern itself has been modeled using the OEDGE interpretive code [8]. The focus of the present paper is on the region near the injection location, also interpreted using the OEDGE code, but with the addition of a module DIVIMP-HC that follows the molecular break-up kinetics (presently using the simple data base of Ehrhardt and Langer [9], preliminary to upgrade to the more exhaustive data base of Janev and Reiter [10]).

Data from the toroidally viewing camera were processed to give 2D reconstructions of the CII (at 514 nm), i.e., $C^+$, and CIII (at 465 nm), i.e., $C^{2+}$, spatial distributions ('clouds'), Fig. 2, top. The reconstruction was made possible by the fact that the injection was toroidally symmetric. It is evident that the CIII is shifted toward the inner divertor, relative to the CII, indicative of entrainment of the carbon in a strong parallel flow along B toward the inside. It is also possible that the transport is a cross-field drift (~poloidal), but the hypothesis here is that the transport is parallel – or *effectively* parallel.

Such fast parallel flows in the main SOL have been reported in other tokamaks, measured for example with Mach probes [11–13]. The driving mechanism has not as yet been identified. Therefore in the OEDGE modeling used here, a value of the parallel flow speed is simply specified (and then varied) as part of the 'plasma background', which is then used as input to the Monte Carlo DIVIMP-HC code. The radial profiles of $n_e$ and $T_e$ are taken from a combination of measurements from

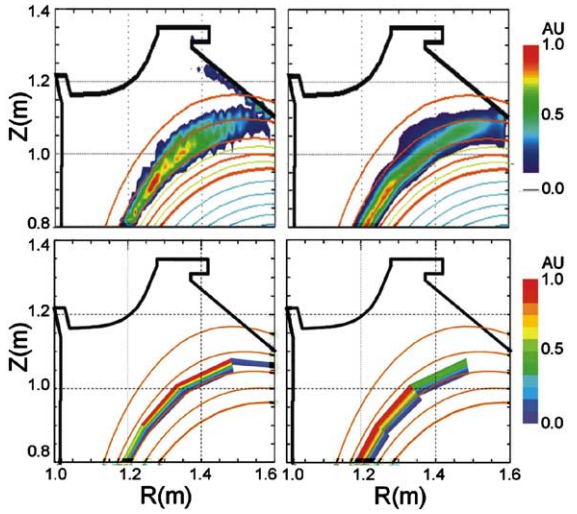


Fig. 2. Reconstructed 2D pictures from the toroidal viewing camera, in CII (top left) and CIII (top right). At bottom the same but for code results, case of $M_{\|} = 0.4$ and $D_{\perp} = 0.3\ m^2/s$. Same color bars for expt and code. The camera pictures are occluded below $Z \sim 0.8$ m.

Thomson scattering (TS) and a reciprocating probe (RCP), Fig. 3, plus an OSM solution generated by Elder [8]; the TS and RCP profiles did not precisely match – perhaps due to EFIT uncertainties – however, small shifts produced good agreement for all three profiles, for both $n_e$ and $T_e$. The 'plasma background' used here is very simple: radial profiles of $n_e$ and $T_e$ (= $T_i$, assumed) that are taken to be constant along the field lines, and a parallel flow speed that is also invariant along the field lines. The parallel flow was specified using a (spatially constant over the whole SOL) Mach Number, $M_{\|} \cdot M_{\|} \equiv v_{\|}/[k(T_e + T_i)/m_D]^{1/2}$, $T_i = T_e$ assumed.

The other main adjustable parameter was the cross-field diffusion coefficient, $D_{\perp}$, also taken to be spatially constant. A large number of OEDGE code runs were made, varying $M_{\|}$ and $D_{\perp}$, searching for the solution which best met the following constraints:

1. Matching the shape and separation of CII and CIII intensity distributions ('clouds') measured by the toroidally viewing cameras, Fig. 2.
2. Matching the poloidal distribution of CIII (at 465 nm) light measured by the absolutely calibrated Filterscope, which viewed the gas injection region from below, Fig. 1.
3. Matching the $C^{6+}$ density increment in the confined plasma, as measured by CER spectroscopy, which indicated a total C-ion density increment just inside the separatrix of $2 \times 10^{16}\ m^{-3} \pm 50\%$.

It is possible to get a qualitative impression of the degree of match between code and the camera 2D CII,

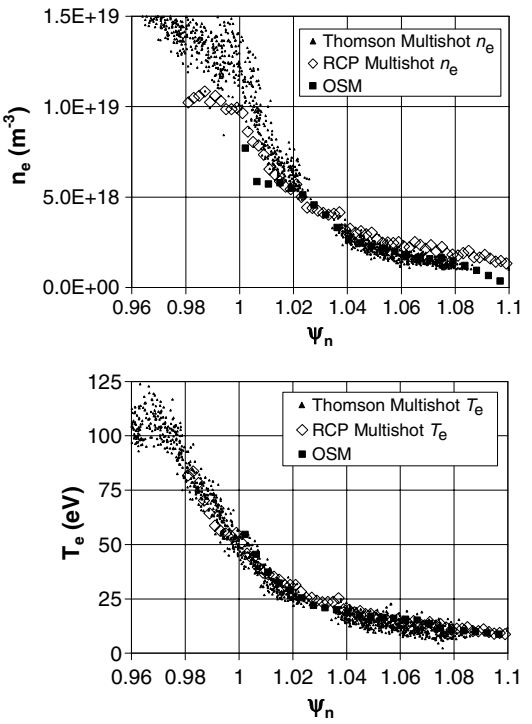


Fig. 3. Profiles of $n_e$ and $T_e$ in the SOL, from [8].

CIII 'clouds' just by looking at the plots. Fig. 2 bottom shows a particular code result ($M_{\|} = 0.4$ and $D_{\perp} = 0.3\ m^2/s$) which reproduces the camera pictures reasonably well, Fig. 2, top. However, in order to make quantitative comparisons, the camera data were processed to produce poloidal profiles (coordinate center at machine center, and poloidal angle measured CCW from vertical), by integrating along the radial lines extending from the machine center. Fig. 4 shows the experimental results for CII and CIII, together with code results for $M_{\|}$ ranging from 0 to 1, all using $D_{\perp} = 0.3\ m^2/s$. As can be seen, the best match is for $M_{\|} = 0.2–0.6$. Similar comparisons were used to establish that $D_{\perp} \sim 0.3\ m^2/s$ gave the best match, although shapes were not strongly dependant on $D_{\perp}$. The same sort of quantitative comparison can be made with the absolutely calibrated filterscope CIII poloidal distribution and in Fig. 5 the experimental results are compared with the code results, again for $M_{\|}$ ranging from 0 to 1, all using $D_{\perp} = 0.3\ m^2/s$. Here the best value of $M_{\|}$ is more sharply indicated to be ~0.4. In a set-up shot, various flow rates were tried, up to levels ~4X that which was finally used in the actual $^{13}CH_4$ injections. The poloidal shapes of the measured filterscope CIII emission was insensitive to the flow rate over this range, indicating that the gas puff is not itself causing the SOL plasma flow, but is providing a valid way to measure the pre-existing flow, i.e., $M_{\|}$.

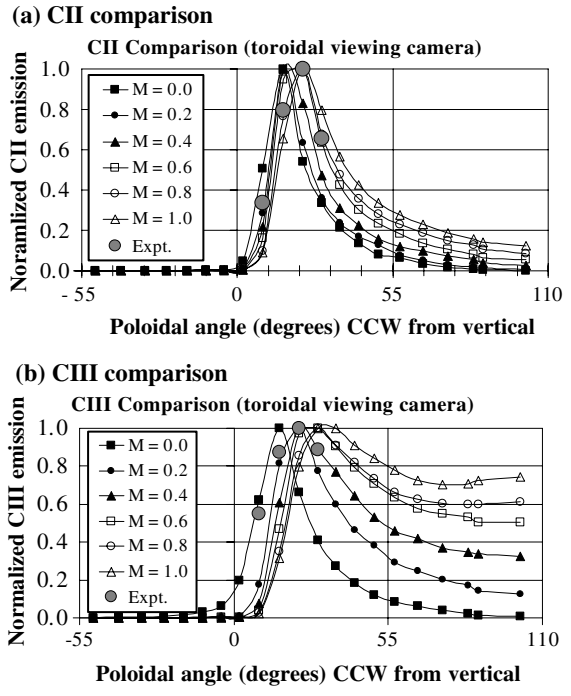


Fig. 4. Comparison of CII and CIII poloidal profiles taken from the 2D reconstructions of the toroidally viewing camera, and code results assuming different values of $M_{\|}$. $D_{\perp} = 0.3\ m^2/s$. All profiles normalized to unity at peak.

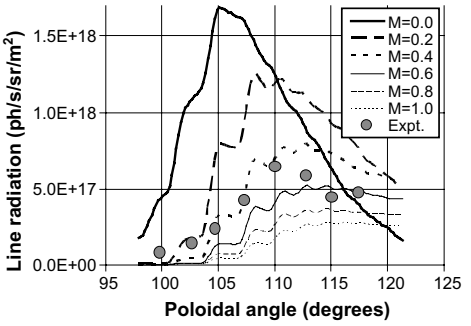


Fig. 5. Comparison of poloidal profile of CIII measured by the upward-looking Filterscope (absolutely calibrated) compared with code results based on various parallel Mach Numbers. $D_{\perp} = 0.3\ m^2/s$.

The values of $M_{\|}$ and $D_{\perp}$ inferred here are close to the values inferred by Elder from his analysis of the $^{13}C$ deposition pattern in the inner divertor [8].

The comparison of the measured C-ion density increment just inside the separatrix, $2 \times 10^{16}\ m^3 \pm 50\%$, and the code values are given in Fig. 6, and indicates a value of $M_{\|} \sim 0.3$. Taking into account the radial profile of the C-ions in the main plasma, from CER, the particle confinement time (i.e., the total core $^{13}C$-ion content divided by the $^{13}CH_4$ puff rate) is found to be $\tau_c \sim 5.5$ ms. This value is fairly close to the values reported by West [14], of ~10 ms, also for $CH_4$ puffing into DIII-D, although using localized wall puffing. The closely related OEDGE modeling of Elder [8] showed that $\tau_c$ would be ~4X higher if the $CH_4$ were ionized at the separatrix, rather than at the actual location, ~3 cm radially outside the separatrix. Thus the main plasma is fairly well shielded from such an external proxy for a wall source of methane – and thus, by implication, for wall chemical sputtered sources.

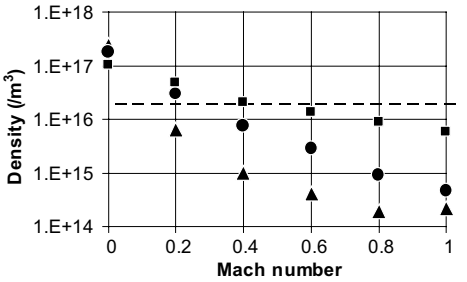


Fig. 6. Carbon density increment at the separatrix calculated by the code, compared with the CER measured value. Dashed line experiment, triangles $D_{\perp} = 0.1\ m^2/s$, circles $D_{\perp} = 0.3\ m^2/s$, squares $D_{\perp} = 1.0\ m^2/s$.

Sticking probabilities for hydrocarbon fragments were approximated from Ref. [15] as: $CH_4$: 100%, $CH_3$: 92%, $CH_2$: 50%, CH: 20%, C: 25%. DIVIMP-HC results showed that only ~25–40% of the puffed $^{13}CH_4$ was locally deposited (as neutral fragments) and most of the injected C reached the $C^+$ and higher states, and was then transported with high efficiency by the fast SOL flow down along the centrepost and into the inner divertor. Thus, so far as being a source of carbon which ends up in co-deposition trapping of H/D/T in the inner divertor – such wall chemical sources can, unfortunately, be quite efficient.

## 3. Conclusion

The molecular breakup of $CH_4$ injected in a toroidally symmetrical way into the main SOL of DIII-D, at a location far from the divertor, has been modeled using the interpretive DIVIMP-HC (OEDGE) code, to extract information from spectroscopic measurements – toroidal cameras, filterscopes and CER – on the SOL (effective) parallel flow speed, the efficiency of carbon contamination of the main plasma and the efficiency of conversion of the puffed $CH_4$ to $C^+$ in the SOL that can end up creating carbon co-deposits in the inner divertor. Although such chemical wall sources of carbon appear to be fairly well shielded from contaminating the confined plasma, the fast parallel flow, together with a

small prompt local loss (by neutral fragment deposition near the $CH_4$ entry into the plasma) means that such sources will be rather efficient at creating carbon H/D/T co-deposits in the inner divertor, in confirmation of the experimental findings in JET [4] and DIII-D [2].

## Acknowledgments

The authors would like to acknowledge the support of a Collaborative Research Opportunities Grant from the Natural Sciences and Engineering Research Council of Canada and the work supported by US DOE Grant and Contract Nos. DE-FC02-04ER54698, W-7405-ENG-48, DE-AC02-76CH03073, DE-AC04-94AL85000, DE-FG02-92ER54139.

## References

[1] J.D. Strachan, W. Fundamenski, M. Charlet, et al., Nucl. Fus. 43 (2003) 922.
[2] S.L. Allen, A.G. McLean, W.R. Wampler, et al., these Proceedings. doi:10.1016/j.jnucmat.2004.09.066.
[3] J. Likonen, S. Lehto, J.P. Coad, et al., Fus. Eng. Des. 66–68 (2003) 219.
[4] J.P. Coad, N. Bekris, J.D. Elder, et al., J. Nucl. Mater. 290–293 (2001) 224.
[5] P.C. Stangeby, J.D. Elder, J.A. Boedo, et al., J. Nucl. Mater. 313–316 (2003) 883.
[6] A.G. McLean, MSc thesis, University of Toronto, 2003.
[7] W. Wampler, S.L. Allen, A.G. McLean, et al., these Proceedings. doi:10.1016/j.jnucmat.2004.10.124.
[8] J.D. Elder, P.C. Stangeby, D.G. Whyte, et al., these Proceedings. doi:10.1016/j.jnucmat.2004.10.138.
[9] A.B. Ehrhardt, W.D. Langer, Collisional processes of hydrocarbons in hydrogen plasmas, PPPL-2477, September 1987.
[10] R.K. Janev, D. Reiter, J. Nucl. Mater. 313–316 (2003) 1202.
[11] S.K. Erents, A.V. Chankin, G.F. Matthews, et al., Plasma Phys. Control. Fus. 42 (2000) 905.
[12] N. Asakura, S. Sakurai, K. Itami, et al., J. Nucl. Mater. 313–316 (2003) 820.
[13] B. LaBombard, S. Gangadhara, B. Lipschultz, et al., J. Nucl. Mater. 313–316 (2003) 995.
[14] W.P. West, C.J. Lasnier, D.G. Whyte, et al., J. Nucl. Mater. 313–316 (2003) 1211.
[15] D.A. Alman, D.N. Ruzic, J. Nucl. Mater. 313–316 (2003) 182.